EPJ Web of Conferences **309**, 04023 (2024) https://doi.org/10.1051/epjconf/202430904023
EOSAM 2024

Spatially resolved refractometry, fluorophore-concentration, axial-position, and orientational imaging using an evanescent Bessel beam

Kaitlin Szederkenyi[1,#], *Carine* Julien[1,#], *Bruno* Lagarde[1], *Ilya* Olevsko[2,3], *Adi* Salomon[1,2,3], and *Martin* Oheim[1,*]

[1] Université de Paris, SPPIN - Saints-Pères Paris Institute for the Neurosciences, CNRS, Paris, France;
[2] Chemistry department, Bar-Ilan University, 529000, Ramat-Gan, Israel;
[3] Institute of Nanotechnology and Advanced Materials (BINA), Bar-Ilan University, 529000, Ramat-Gan, Israel.

Abstract. Simultaneous field- and aperture-plane (back-focal plane, BFP) imaging enriches the information content of fluorescence microscopy. In addition to the usual density and concentration maps of sample-plane images, BFP images provide information on the surface proximity and orientation of molecular fluorophores. They also give access to the refractive index of the fluorophore-embedding medium. However, in the high-NA, wide-field detection geometry commonly used in single-molecule localisation microscopies, such measurements are averaged over all fluorophores present in the objective's field of view, thus limiting spatial resolution and specificity. We here solve this problem and demonstrate how an oblique, variable-angle, coherent ring illumination can be used to generate a Bessel beam that - for supercritical excitation angles - produces an evanescent needle of light. Scanning the sample through the this evanescent needle enables us to acquire combined sample-plane and BFP images with sub-diffraction resolution and axial localisation precision. Background, resolution and polarisation considerations will be discussed.

1 Introduction

Back-focal plane (BFP) imaging is common to approaches like conoscopy, Müller-matrix polarimetry [1], single-molecule orientational imaging [2,3] or near-interface sensing [4]. More recently, BFP image analysis and filtering approaches have been combined with high-numerical aperture (NA) objectives for single-molecule localisation microscopies (SMLMs) using supercritical angle fluorescence (SAF) detection. SAF provides a complement to total internal reflection fluorescence (TIRF) [5,6], notably for axial single-molecule localisation [7], and for the disambiguation of intensity changes from molecules or fluorescently labelled organelles moving along z [8].

Beyond imaging, SAF-based techniques have garnered interest for thin-film characterisation [8] and for *in situ* refractometry [9,10]. The segmentation of BFP images and their decomposition into SAF and under critical fluorescence (UAF) emission components allows for the sensitive measurement of the fluorophore height (via the SAF/UAF intensity ratio), and of the local refractive index (RI, via the measurement the emission critical angle).

A downside of wide-field detection is that the resulting measurements are averages over all fluorophores excited and within the field-of-view of the objective. In biological SAF refractometry, an alternative strategy has therefore been to address fluorophores to specific subcellular locations, either through site-specific labelling or via genetic targeting strategies [9]. Nevertheless, BFP images and the parameters derived thereof suffer from a limited spatial resolution and typically represent ensemble averages over areas several μm^2 wide.

We here report on our ongoing work using an evanescent Bessel beam in a sample-scanning geometry for providing highly resolved intensity and RI-maps.

2 Experimental details

We built an inverted microscope for variable-angle hollow-cone illumination from optical bench components, **Fig. 1a**. Briefly, the linearly polarised beam of an yellow HeNe laser (594 nm, MellesGriot) was passed through a radial polarisation converter (ARCoptics), expanded and the Gaussian beam profile converted into a coherent ring using a dual-axicon telescope. An additional converging lens focused the ring beam in the BFP of an αPlan-Apo-chromat x100/NA1.57 Oil-HI DIC Corr M27 TIRF objective (ZEISS). This ensemble allowed for a variable beam expansion (when moving the axions) and variable focussing (when moving the focusing lens, FL). With the used Immersol HI 661 oil (n_2=1.661 at 23°C) and sapphire coverslips (n_3=1.768), rings with radii $r_c > f \cdot n_1$ are super-critical and generate an evanescent Bessel beam [11]. Here, n_1 is the RI of the sample or-more precisely - the local, fluorophore-embedding medium. The generated fluorescence was collected through the same objective, extracted with a 3-mm thick dichroic (AHF) and narrowed down with a 594-nm longpass filter. BFP images were collected on an electron-multiplying charge-coupled device (EMCCD) camera (Princeton).

* Corresponding author: martin.oheim@u-paris.fr ; # equal contribution

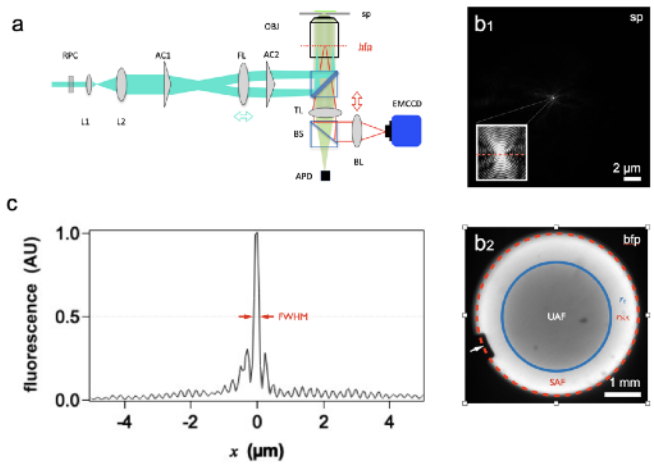

Fig. 1. *Generation of an evanescent Bessel beam.* (a), schematic optical layout. RPC - radial polarisation converter, L- lens, AC- axicon, FL- focussing lens, TL- tube lens assembly, OBJ- objective, BS- beam splitter, APD - avalanche photodiode, BL - Bertrand lens, EMCCD - electron-multiplying charge-coupled device, sp -sample plane, bfp - back focal plane. (b), example images; b_1, sample-plane (sp) image of the generated illumination pattern in a homogenous thin fluorescent film; *inset* magnified view of the central spot; b_2, corresponding bfp image. *Red* and *blue* circles identify the objective pupil (r_{NA}) and the radius corresponding to the emission critical angle, $r_c = f \cdot n_1$, respectively, used for the segmentation of SAF and UAF emission components. White arrow identifies the displaceable segment diaphragm of the ZEISS objective. (c), intensity line profile along the red-dashed line on panel b_1,witnessing the Bessel-beam profile. FWHM size of the central peak was 147±3 nm.

Results

Supercritical illumination with a coherent, radially polarised hollow cone of light produced an evanescent Bessel beam that was recognised by its characteristic intensity pattern when imaging a homogenous, orange-emitting fluorescent film (exposed to air). The SP image, **Fig.1b1**, reveals a narrow, high-intensity peak, with a full-width half-axial (FWHM) diameter of 147±3 nm, surrounded by a lower-intensity concentric ring pattern. The corresponding BFP image, taken with the Bertrand lens in place, **Fig.1b2**, shows the expected isotropic radiation pattern, with a the transition between under- (UAF) and supercritical fluorescence (SAF) emission components at r_c = 1.65 mm (*blue* circle, NA_c = 1.0).

The outer diameter provides an estimate of the effective NA_{eff} of the used objective of 1.574, close to its specified value of 1.57 (*red*).

We next imaged a nanoscale sandwich featuring a far-red emitting dye layer at 105 nm fluorophore height, as verified by SAF/UAF ratiometry [8], with a ratio $R = I_{SAF}/I_{UAF}$ = 0.32 (compared to 0.49 for the same dye at z = 0), We verified that the Bessel-beam illumination was confined in z by varying the incidence angle and validating the characteristic intensity curve. We conclude that, indeed, we generated an evanescent needle of light.

Perspective

While our bench top experiment provides a successful proof-of-concept, several points merit improvement:

- while inexpensive and simple, the built three-lens telescope is somewhat awkward to align, even with a very-high NA objective and sapphire coverslips used here, a combination which offers more “space” for supercritical light than the more common x100/ NA1.46 objective and borosilicate glass (BK-7) coverslips;
- surprisingly the effect of circular polarisation from the RPC is not as strong as expected, perhaps due to the depolarising effect of the very high-NA objective ;
- while the evanescent needle of light provides the expected sub-diffraction spot, quite some energy is lost in the surrounding ring pattern. In fact, the concentric rings are sufficiently intense for fluorescence excitation, and this feature has earlier been used for flat-field illumination in TIRF microscopy [11]. In this work the authors ignored the tiny central high-intensity spot ;
- the problem of background excitation should be resolved by 2-photon excitation TIRF [12, 13], due to the quadratic intensity dependence of the excited fluorescence, or by adding a confocal pinhole or image-scanning microscopy honeycomb detector, centred on the central peak of the Bessel beam.

References

1. A. B. Vasista, D. K. Sharma, G.V. Pavan Kumar, Enc Appl Phys (2019) https://doi.org/10.1002/3527600434.eap817
2. M. Böhmer, J. Enderlein, J Opt Soc. Am B **20**, 554-9 (2003)
3. M. A. Lieb, J. M. Zavislan, and L. Novotny, J Opt Soc Am B **21**, 1210-15 (2004)
4. T. Ruckstuhl, S. Seeger, Opt Lett **29**(6), 569-71 (2004)
5. M. Brunstein, A. Salomon, M. Oheim, ACS Nano **12** 11725-30 (2018)
6. M. Oheim, A. Salomon, M. Brunstein, Biophys J **118**, 2339–48 (2020)
7. N. Bourg, *et al.*, Nat. Photonics. **9**, 587–593 (2015)
8. H. Klimovsky, *et al.* Adv Opt Mater **11**(14): 2203080 (2023)
9. M. Brunstein, L. Roy, M. Oheim, Biophys J **112**(9), 1940-8 (2017)
10. B. Ferdman, *et al.*, ACS Nano **12**(12), 11892–8 (2018)
11. B. Schreiber, K. Essayed, K. G. Heinze, Opt Lett 42(19), 3880-3 (2017)
12. F. Schapper, J. T. Gonçalves, M. Oheim, Eur Biophys J, **32**, 635–43 (2003)
13. M. Oheim, F. Schapper, J Phys D: Appl. Phys. **38** R185 ()